COUPLING STRATEGY OF HVAC SYSTEM SIMULATION AND CFD PART 1: STUDY ON THE DESIGN PHASE OF AN UNDER FLOOR AIR DISTRIBUTION SYSTEM

Gyuyoung Yoon[1], Junya Kondo[2], Yuka Sakai[3]
Takeshi Watanabe[4], Satoru Iizuka[5], Masaya Okumiya[5]
[1]Nagoya City University, Nagoya, Japan, [2]Kajima Corporation, Tokyo, Japan
[3]Toyama City Hall, Toyama, Japan
[4]NTT Facilities, Tokyo, Japan, [5]Nagoya University, Nagoya, Japan

ABSTRACT

This report describes the utility of coupling an energy simulation tool and computational fluid dynamics (CFD) for modelling a heating, ventilation and air-conditioning (HVAC) system, and demonstrates the application of this method in the design phase. A case study was conducted for the design phase of an air-conditioning system with an under floor air distribution system.

First, the cooling load for the target room was estimated, and the air-handling unit was designed based upon the estimated peak load. Next, the cooling load of the chilled water (air-conditioning load) was estimated first by using the energy simulation tool alone, and then by using the energy simulation tool coupled with CFD.

We found that it was possible to estimate the proper air-conditioning load when the actual air-temperature distribution of the room was modelled by CFD.

INTRODUCTION

The design of heating, ventilation and air-conditioning (HVAC) system has focused upon systems that can withstand the peak building load. However, the required building load accounts for less than half of the peak load during most of the operating period.

On the other hand, partial loads lead to poor HVAC system operational efficiency. Thus, an energy simulation that allows for a seasonal performance evaluation that considers the efficiency drop when a system operates at partial load is expected to promote proper system design, construction and operation.

For most HVAC system energy simulations of a building, including building heat load calculations, the air-conditioned space is assumed to have complete mixing with evenly distributed air temperature and air humidity; therefore, the simulated space differs from an actual space.

When designing a system to improve air-conditioning efficiency by localising the target area of environmental control, the difference of distributed air temperature and humidity between the actual space and the simulated space becomes large.

Although dividing the air-conditioned space into residential and non-residential areas can reduce the difference, when each space is assumed to be completely mixed, the simulated performance and energy consumption of the HVAC equipment will be different from the actual results. Energy simulation coupled with CFD should be a useful method for eliminating this difference and realistically modelling an actual system.

This study aims to support energy management throughout the life cycle of a building's HVAC system by investigating energy simulation coupled with CFD.

By conducting an energy simulation that uses the air-temperature and air-flow distributions obtained through CFD analysis of the space, we aim to improve the accuracy of the simulation and to adequately reproduce the behaviour of the system. In addition, we aim to demonstrate that the method of coupling CFD and energy simulation is useful for system design, construction and operation.

The idea of using CFD as the boundary conditions in energy simulation has been studied before. Lam et al. (2001) used the air-temperature and air-flow distributions obtained by CFD to optimise a gym HVAC system.

Zhai et al. (2003, 2005, 2006) verified the accuracy of the coupled method and performed a sensitivity analysis. Zhung et al. (2006) designed a gym HVAC system by using the coupled method. Iida (Iida et al., 2008) showed that the coupled method is useful in the diagnosis and control of an HVAC system.

In the present paper, the applicability of the coupling method is discussed in terms of life cycle energy management for a building, and a case study assuming an underfloor air distribution (UFAD) system shows that the coupled method is useful for estimating the actual cooling load for an air-handling unit (AHU). In addition, the effect on the energy consumption of the difference between the actual air-conditioning load and the design load is shown.

METHOD OF COUPLING ENERGY SIMULATION AND CFD

Essentials for the coupled method

In the design phase, the method of coupling energy simulation and CFD is useful for accurately estimating the cooling and heating loads, as well as the peak and partial loads, whilst predicting the actual air-temperature and air-flow distributions in the space.

In the construction phase, the coupled method can be used for system tuning. In the operation phase, the thermal environment of the space and the system performance can be reproduced by using the coupled method. Then, the method can be applied to supporting the control and fault detection of an HVAC system.

Figure 1 shows the assumed boundary conditions of the coupled method. There are two boundary condition cases: one is the case coupled on the air side and the other is the case coupled on the water side. The first case couples energy simulation with CFD modelling of the supply air temperature, the return-air temperature, the humidity and the air volume of the AHU. This case is the technique adopted in this study. The other case is coupled at the chilled water temperature and water volume of the cooling coil. These two types of cases can be selected from boundary conditions that can be handled by the energy simulation tool.

Figure 2 shows the calculation cycle for carrying out the energy simulation coupled with CFD. We will now describe the case study conducted in this paper: first, CFD calculations are conducted for air temperature and air flow in the space, with the initial value of supply-air temperature taken at point 1 in Figure 2; next, the energy simulation extracts the supply-air temperature for the next time step. This represents one cycle in the process of energy simulation coupled with CFD. After the first coupled calculation, the CFD calculation can progress with the supply-air temperature obtained from the energy simulation.

In most cases, the coupled calculation is conducted with the assumption that the energy simulation converges within a constant time step (empirically 1 h) corresponding to the step response. From this assumption, a coupled time step of 1 h for a cycle is adequate. In addition, it would be possible to take the coupled time step shorter than 1 h, if the energy simulation can handle dynamic calculations or neglect dynamic system behaviour.

In this paper, the Life Cycle Energy Management (LCEM) tool (Version 3.02) is used for the energy simulation, and STREAM (Version 8) is used for the CFD analysis. The LCEM tool is useful for life cycle energy management, and was developed by the Ministry of Land, Infrastructure, Transport and Tourism. The LCEM tool was validated in a previous study (Ito et al., 2008).

CALCULATION CONDITIONS OF ENERGY SIMULATION COUPLED WITH CFD

Case study outline

In this study, energy simulation coupled with CFD is used to design the HVAC system of a model building. Cooling loads corresponding to the three cases shown in Table 1 are estimated, and then the usefulness of energy simulation coupled with CFD is discussed.

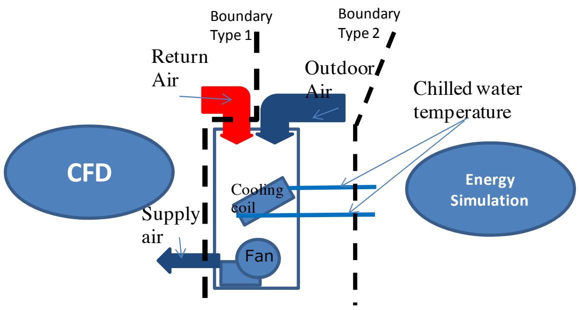

Figure 1: Boundary conditions of the coupled energy simulation and CFD calculations

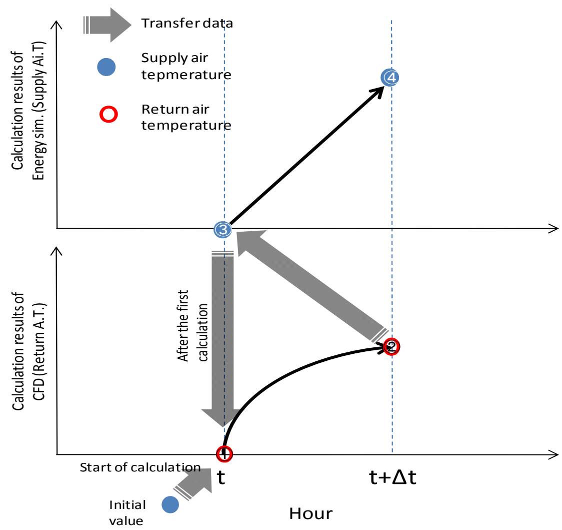

Figure 2: Diagram of the coupled calculation cycle

Table 1: Case study description

Case	Details and description
Case 0	Assuming a completely mixed zone (Uniform air-temperature distribution) - Air distribution on ceiling - No coupled calculations
Case 1	Assuming two completely mixed zones (Uniform air-temperature distribution in each zone) - Underfloor air distribution - No coupled calculations
Case 2	Considering air distribution in the zone - Underfloor air distribution - Coupled calculations

Case 0 represents a typical air distribution system, which has air outlets in the ceiling. Cases 1 and 2 represent UFAD systems, which have air outlets in the floor. The mixed-air system of Case 0 is designed to air-condition the entire space; Cases 1 and 2 are designed to air-condition only the residential area, not the non-residential area.

We can consider Case 0 to be a completely mixed space having a uniform air-temperature distribution, which is a general assumption in the empirical HVAC design process.

In Cases 1 and 2, the air-temperature distribution in the space is taken into account in different ways. Case 1 considers just two air layers: the residential layer and the non-residential layer. Case 2 takes into account the linear air-temperature distribution like that found in an actual space.

Outline of the HVAC system of the model building

The model building is a nine-storey, reinforced concrete (RC) office building located in Tokyo, Japan. As shown in Figure 3, the typical floor of this building has an area of 1,144 m^2, and consists of two office zones and a core zone located in the centre of the floor. The two office zones have window-mounted air-flow-window systems installed on the north and south sides of the building.

Each office zone is divided into four subzones: N1 through N4, and S1 through S4. Two of the subzones are air-conditioned by one AHU. There are four AHUs per floor. Table 2 shows the heat load conditions for the internal heat gain and the air-flow-window system.

Figure 4 shows the HVAC system diagram of the model building for Cases 1 and 2. The AHU intakes a mixture of outdoor air and return air, and discharges air under the floor with a constant air volume in Cases 1 and 2, whereas in Case 0, the AHU discharges air to an air distributor mounted on the ceiling.

The air-flow window is ventilated with air discharged by the AHU in Cases 1 and 2, whereas in Case 0, it is ventilated with room air sucked into the opening of the air-flow window, installed near floor level.

Figure 5 shows a diagram of the LCEM tool framework for the HVAC system simulation of the model building. The framework consists of six components: the secondary tank, the cooling coil, the fan, the duct, the CAV unit and the room. Within this framework, we can obtain the chilled water temperature and the chilled water volume which correspond to the cooling load of the room.

Figure 6 shows the CFD model of the target space. The CFD model is used for only one zone, S3, to reduce the calculation load. The rectangular solids in the CFD model represent tables, chairs and people in the office. Table 3 shows the CFD calculation conditions. The turbulence model is adapted from the RNG k-e model, which has been validated in previous studies (Tominaga et al., 2009; Sun et al., 2007).

The cooling load calculations for Cases 0 and 1 are shown in Figure 7. The cooling loads were obtained by using Micro-HASP/TES for Windows. The heat load calculation for Case 1 was conducted under the assumption that the room had two zones: the residential zone and the non-residential zone. The residential zone spans from floor level to a height of 1.7 m.

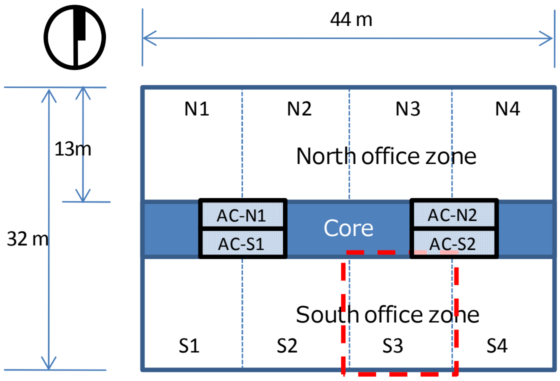

Figure 3: Typical plan view of the model building

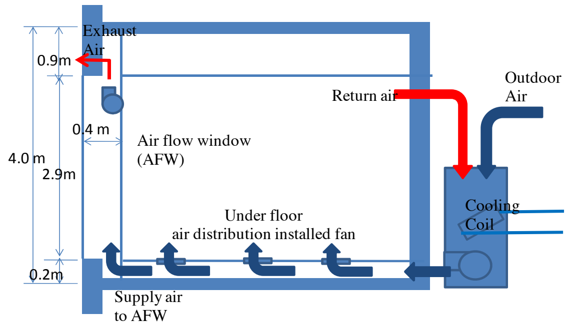

Figure 4: Diagram of the air system around the AHU

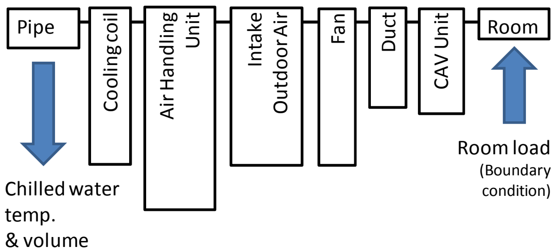

Figure 5: Diagram of energy calculation (LCEM tool) framework

Table 2: Heat load conditions

Resident density		0.10 people/m^2
Lighting (semi-embed on ceiling)		20 W/m^2
Outlets and Office machines		20 W/m^2
Outdoor air intake per resident		25 m^3/h
Thermal characteristic of AFW	SC value	0.28
	U value	2.08 W/m^2K

The peak cooling load occurs at 12:00 on September 11. The peak load for Case 0 is 21.9 kW (20.1 kW sensible heat load), and for Case 1 is 21.1 kW (19.3 kW sensible heat load: 13.9 kW for the residential area and 5.4 kW for the non-residential area). On the basis of the peak cooling loads for Cases 0 and 1, we designed the cooling coil and AHU for each case.

Table 4 shows the HVAC system properties for each case. We determined the HVAC system properties for Case 2 to be the same as those for Case 1. The supply-air temperatures for the AHU were determined to be 15 °C in Case 0 and 18 °C in Case 1. The mixing air temperature of the AHU intake was determined to be 26 °C in Case 0 and 29.1 °C in Case 1.

The mixing air temperature of 29.1 °C for Case 1 is the same as the air temperature of the non-residential area obtained from heat load calculations.

Detail of energy simulation and CFD

The energy simulation had two load conditions: the peak load condition of September 11 and the partial load condition of April 12, each simulated for 10 h/day from 8:00 to 17:00. Table 5 shows the boundary conditions for each case.

In Cases 0 and 1, we ran the energy simulation with the room load obtained from the heat load calculations described above. In Case 2, we ran the energy simulation coupled with CFD instead of applying the room load.

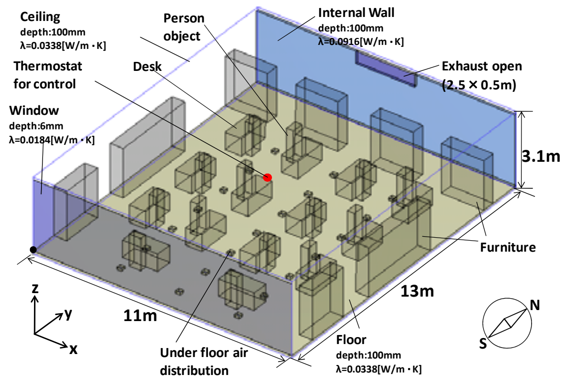

Figure 6: CFD Calculation domain of the room (only the S3 zone shown in Figure 3)

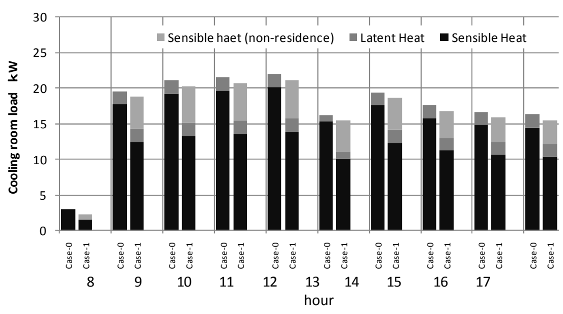

Figure 7: Cooling load for Cases 0 and 1 on September 11

Table 3: Calculation conditions of CFD

Grid points	86(x)×102(y)×24(z)=210,528
Scheme for convection terms	1st order upwind scheme for all governing equations
Turbulence model	Standard k-ε model
Inlet boundary condition	Velocity : 0.91 m/s Temp. : 14 to 22 °C by LCEM tool Humidity : 80% rh to 90% rh by LCEM tool k : 0.0069 m^2/s^2 ε : 4.68×10^{-3} m^2/s^3
Outlet boundary condition	Zero-gradient conditions for all variables
Wall boundary condition*1	Velocity : Logarithmic law Temp. : Logarithmic law for Over all heat transfer except the boundary of east and west wall Humidity : No vapour transfer
Heat gain object	Light: 20 W/m^2 - Apply on ceiling 10 W/m^2 as convection heat gain - Apply on floor 10 W/m^2 as radiation heat gain Office machine: - OA: 20 W/m^2 - Apply on each desk 204.3 W Person -Apply 55 W as sensible heat -Apply 63W as latent heat equal to water vapour of 0.025 g/s

*1 The window, internal wall, ceiling and floor are the solid considering the thermal conduction. The outer surfaces of these walls, boundary of calculation domain are adiabatic boundary except window. The outer surface of window is given by the outdoor air temperature and the heat transfer coefficient, 23W/m^2K.

Table 4: AHU Properties

Case 0	Cases 1 and 2
	Underfloor type
Cooling cap.: 32.0 kW	Cooling cap.: 30.7 kW
Front area: 0.532m^2	Front area: 0.532m^2
Num. of tubes: 20 per row	Num. of tubes: 20 per row
Num. of row: 5 (HF)	Num. of row: 4 (HF)
Air volume: 5,600 m^3/h	Air volume: 5,600 m^3/h
Outdoor air: 715m^3/h	Outdoor air: 715m^3/h
Chilled water	Chilled water
volume: 93.1 l/min	volume: 88.0 l/min
Temp.: 7-12°C.	Temp.: 7-12°C.
Fan power: 0.95 kW	Fan power: 0.95 kW

Table 5: Boundary conditions for energy simulation

CASE	Boundary conditions
Case 0	Outdoor air temp. and humid. Room load (Sensible and latent heat)
Case 1	Outdoor air temp. and humid. Room load (Sensible and latent heat) Air temp. of non-residence area*1
Case 2	Outdoor air temp. and humid. Return air temp. and humid. Air temp. in room *2

*1 Air humidity of non-residential area is same as residence area
*2 This value is the air temperature of the thermostat, which is used to control the supply-air temperature

Figure 8 shows the calculation flow diagram for the energy simulation coupled with CFD. The coupling of energy simulation and CFD occurs on the air side of the HVAC system; the energy simulation and CFD will input and output the status of the supply and return air. The energy simulation passes the supply-air temperature and supply-air humidity of the AHU to the CFD calculation. Then, CFD will simulate the air-temperature and air-flow distribution of the space, and output the return-air temperature and return-air humidity, as well as the thermostat setting required in order to control the supply-air temperature. This series of processes is repeated at 30 s intervals, as we assume that the dynamic behaviour of the cooling coil can be neglected in this study. The supply-air temperature range of the AHU is from 14 °C to 22 °C, and the proportional range for room-temperature control is from 24 °C to 28 °C. The thermostat sensor is located in the centre of room at a height of 1.7 m.

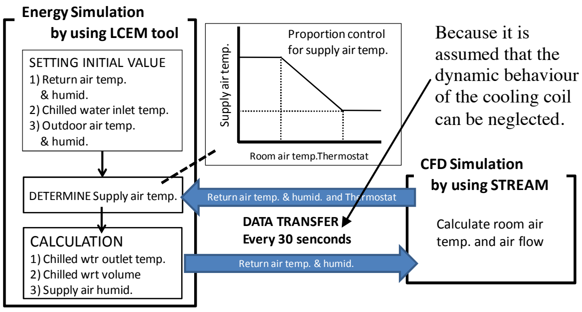

Figure 8: Coupled calculation flow

SIMULATION RESULTS

Comparison of cooling load for coils on peak day

Figure 9 shows the air-conditioning load for each case: September 11 and April 12. Energy simulation using the LCEM tool provided the air-conditioning load, the chilled water temperature and the chilled water volume. The cooling load is represented by the room load, which is the rate of heat removed from the room and the fresh-air load. A negative value of the fresh-air load is found on April 12 because a cooling effect can be obtained by inducing fresh air.

The air-conditioning loads during the peak condition, September 11, are 227.2 kWh, 203.8 kWh and 197.3 kWh for Cases 0, 1 and 2, respectively; the room loads, excluding the fresh air load, for Cases 0, 1 and 2 are 172.6 kWh, 165.5 kWh and 153.5 kWh, respectively.

The cooling load for Case 1 is smaller than that for Case 0 because Case 1 does not include cooling of the non-residential area.

The cooling load for Case 2 is 6.9% smaller than that for Case 1. The difference between Case 1 and Case 2 can be described by using the air-temperature distribution in the space.

Figure 10 shows the air-temperature distribution simulated by CFD for September 11 at 12:00. The lower temperature zone exists from floor level to a height of 1.0 m, and is generated by the air flow from UFAD. The top of the space is at a higher temperature because of the ascending flow induced by heat released from the office machines and residents. For these reasons, thermal stratification occurs in the space. The thermal stratification shown in Figure 10 does not exist in the Case 0 and Case 1 spaces, which are assumed to have completed mixing. As shown in Figure 11, the vertical distributions of air temperature in the space are different in each case. Cases 1 and 2 have a difference in air temperature between the top and bottom of the space, whereas

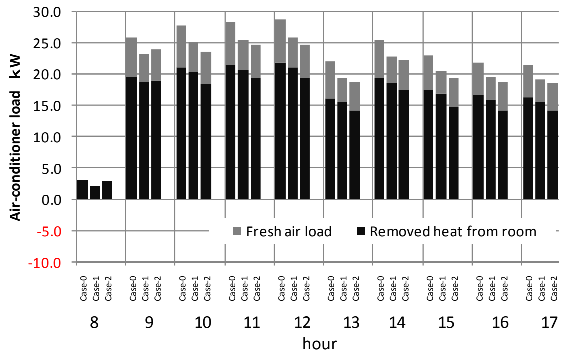

(a) September 11

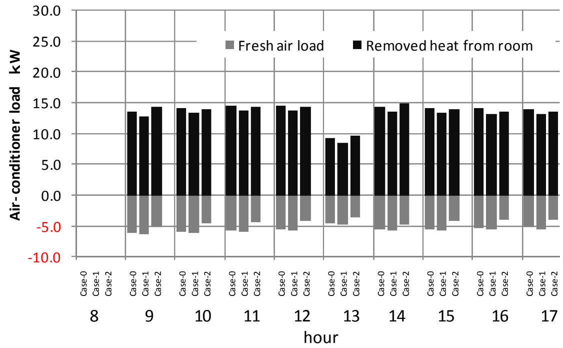

(b) April 12

Figure 9: Air-conditioning load for each case

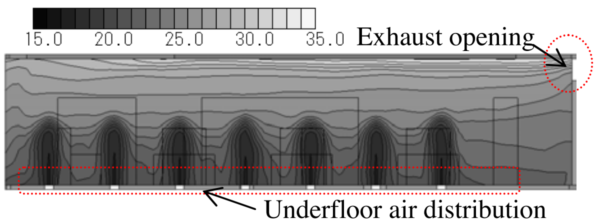

Figure 10: Air-temperature distribution (September 11, 11:00, x=5.5 m)

Case 0 has a uniform air-temperature distribution. Also, the gradient of the air-temperature distribution is steeper in Case 2 than in Case 1.

Table 6 shows the air temperature and air humidity of the room for each case at a point in the centre of the room, 1.7 m above floor level. Table 7 shows the supply-air and return-air temperatures for the AHU in each case.

The air temperature of the room for Cases 0 and 1 is maintained at a set point of 26 °C during the entire simulation; however, the air temperature of the room in the Case 2 differs little from the temperature setting, except at 8:00.

In Cases 0 and 1, the air temperature of the room was assumed to be controlled ideally, such that it could be maintained at the set point. On the other hand, Case 2 simulated the air temperature of the room by using CFD, which took into account the offset from the proportional control. The air temperature of the room in Case 2 was 23 °C at 8:00 because the supply-air temperature was 22 °C, which was the upper limit, and there was little heat load at the time.

The dry air humidity in the room was 52.8%, 61.6% and 63.8% for Cases 0, 1 and 2, respectively. Since the supply-air temperature was higher, the air humidity of the room was higher in Cases 1 and 2 than in Case 0.

We found the air-conditioning loads ranged from smallest to largest in the order of Case 2, Case 1 and Case 0, as shown in Figure 9(a), because of the differences in air-temperature distribution for each case, and the differences in supply-air temperature, which can lead to a different latent heat load capacity.

Comparison of the air-conditioning load on an off-peak day

The daily air-conditioning loads in the off-peak case on April 12 are 75.2 kW, 64.1 kW and 85.2 kW for Cases 0, 1 and 2, respectively. The daily air-conditioning load for each case ranged, from smallest to largest, in the order of Case 1, Case 0 and Case 2, a different order than for the peak load condition.

The cooling load of the coil in Case 2 is smaller than that in the other cases because the air temperature of the room in Case 2 is the lowest (Table 8).

Consequently, during the partial load day, the air-conditioning load decreases along with the reductions in room load. However, the degree of the decrease of the air-conditioning load differs depending upon whether the air-temperature distribution is considered. Figure 12 shows the fluctuation of the chilled water temperature and the water volume during the peak load day. The chilled water temperature and water volume differ in each case, owing to the differences in the coil cooling load, and in the mixed air temperature and air humidity introduced into the cooling coil.

In the previous section, the differences in air-conditioning load in each case were confirmed to occur because of the different air-temperature distributions. The differences in the mixed air temperature and mixed air humidity occurred because of the differences in return-air temperature and return-air humidity from the room.

The chilled water volumetric flow rate during the peak load day was 413 L/min in Case 0, 332 L/min in Case 1 and 367 L/min in Case 2. The volume of chilled water affects the electric power consumption of the chilled water pump. The actual volume of chilled water can be obtained via coupling with the CFD simulation because CFD can reproduce the air-temperature distribution of the actual space.

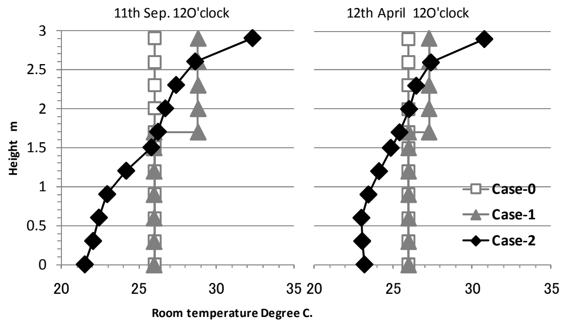

Figure 11: Air-temperature distribution along the vertical direction

Table 6: Air temperature and air humidity in the room on September 11

	Case-0		Case-1		Case-2	
Hour	Temp.*2	Humid.	Temp. *2	Humid.	Temp.	Humid.
8:00-8:59	26.0	45.6	26.0	45.6	23.0	84.9
9:00-9:59	26.0	52.6	26.0	62.5	25.8	59.8
10:00-10:59	26.0	50.1	26.0	60.7	25.5	60.4
11:00-11:59	26.0	49.4	26.0	60.2	25.9	57.5
12:00-12:59	26.0	48.8	26.0	59.7	26.2	56.6
13:00-13:59	26.0	56.1	26.0	66.3	25.6	65.0
14:00-14:59	26.0	53.0	26.0	62.7	25.6	61.2
15:00-15:59	26.0	56.2	26.0	65.0	25.4	63.4
16:00-16:59	26.0	57.8	26.0	66.2	25.1	64.8
17:00-17:59	26.0	58.6	26.0	66.7	25.1	64.9

*1 Air temperature and air humidity of the room are taken at the thermostat, which is located in the centre of the room in each case.
*2 These values are not calculation results.

Table 7: Supply-air and return-air temperature on September 11

	Case-0		Case-1		Case-2	
Hour	Supply	Return	Supply	Return	Supply	Return
8:00~8:59	24.8	25.2	22.0	26.0	26.4	24.8
9:00～9:59	17.1	19.5	18.5	26.0	28.4	27.4
10:00～10:59	16.3	19.0	19.0	26.0	28.7	28.3
11:00～11:59	16.1	18.9	18.3	26.0	28.8	28.0
12:00～12:59	15.9	18.8	17.7	26.0	28.9	28.1
13:00～13:59	18.4	20.7	18.8	26.0	28.3	27.3
14:00～14:59	17.2	19.6	18.8	26.0	28.4	27.3
15:00～15:59	18.2	20.2	19.3	26.0	28.0	26.8
16:00～16:59	18.7	20.5	19.8	26.0	27.8	26.4
17:00～17:59	18.9	20.6	19.8	26.0	27.7	25.5

* Air temperature and air humidity of the room are taken at the thermostat, which is located in the centre of the room in each case.

Table 8: Air temperature and air humidity in the room on April 12

	Case-0		Case-1		Case-2	
Hour	Temp.*2	Humid.	Temp.*2	Humid.	Temp.	Humid.
8:00-8:59	26.0	50.0	26.0	50.0	22.4	83.2
9:00-9:59	26.0	46.1	26.0	46.1	25.2	66.0
10:00-10:59	26.0	47.7	26.0	47.7	25.1	65.6
11:00-11:59	26.0	49.1	26.0	49.1	25.2	65.1
12:00-12:59	26.0	50.0	26.0	50.0	25.4	64.1
13:00-13:59	26.0	43.5	26.0	43.5	24.5	72.6
14:00-14:59	26.0	50.9	26.0	50.9	25.3	64.9
15:00-15:59	26.0	50.9	26.0	50.9	25.2	65.2
16:00-16:59	26.0	50.0	26.0	50.0	25.2	65.7
17:00-17:59	26.0	49.1	26.0	49.1	25.4	65.0

*1 Air temperature and air humidity of the room are taken at the thermostat, which is located in the centre of the room in each case.
*2 These values are not calculation results.

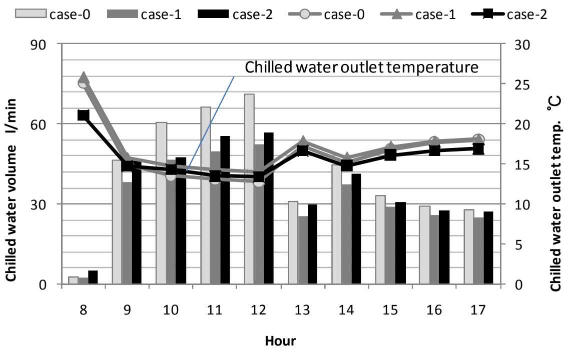

Figure 12: Chilled water volumetric flow rate and water temperature on September 11

CONCLUSION

This case study was conducted to demonstrate the utility of energy simulation coupled with CFD. The case study concerned the evaluation of cooling load for a coil in the design phase of a UFAD system proposed for a model building. Both energy simulation coupled with CFD, and energy simulation alone, were used to model the air-conditioning load.

It was confirmed that the air-conditioning load of the coil differed depending upon whether the energy simulation was coupled with CFD. Also, the air-temperature distribution in the space and the effect of the AHU supply-air temperature led to the differences in cooling load.

On the peak load day, the coupled simulation estimated smaller air-conditioning load values than the non-coupled simulation. On the partial load day, the coupled simulation estimated larger air-conditioning load than the non-coupled simulation. This signifies that the coupled simulation can be used to estimate the cooling load with greater accuracy, and that we can design a more suitable HVAC system capacity that takes into account the actual air-conditioning load.

In the future, we plan to verify the accuracy of the coupled simulation and to study the usability of coupled simulations in the system construction and operation phases.

REFERENCES

Iida, R., Shiraishi, Y., Sagara, N. 2008. Study on control and diagnosis of HVAC systems for an office space, Part 3, Case studies for coupled simulation of CFD analysis and HVACSIM+(J), Summaries of technical papers of Annual Meeting Architectural Institute of Japan, D-2, 1379-1380 (in Japanese).

Ito M. 2008. Development of HVAC system simulation tool for life cycle energy management Part 1 Building Simulation Volume 1, Number 2, 178-191

Lam, J.C., Chan, A.L.S. 2001. CFD analysis and energy simulation of a gymnasium, Building and Environment, 36, 351-358.

SHASE of Japan 2010. Handbook of JSHRAE vol. 13

Sun H., L. Zhao, Y. Zhang 2007. Evaluating RNG k-[epsilon] models using PIV data for airflow in animal buildings at different ventilation rates, ASHRAE Transactions

Tominaga Y. T. Stathopoulos 2009. Numerical simulation of dispersion around an isolated cubic building:Comparison of various types of k–3 models, Atmospheric Environment 43, 3200-3210

Zhai Z., Q. Chen 2005. Performance of coupled building energy and CFD simulations, Energy and Buildings 37, 333–344

Zhai Z., Q. Chen 2003. Solution characters of iterative coupling between energy simulation and CFD programs, Energy and Buildings 35, 493-505

Zhai Z., Q. Chen 2006. Sensitivity analysis and application guides for integrated building energy and CFD simulation/ Energy and Buildings 38, 1060–1068

Zhung .M. et al 2006. Under floor return system of HAVC in a large Gymnasium, Part 3. Annual meeting of AIJ